AN ANALYTICAL APPROACH TO SOUND FIELD REPRODUCTION WITH A MOVABLE SWEET SPOT USING CIRCULAR DISTRIBUTIONS OF LOUDSPEAKERS

Jens Ahrens and Sascha Spors

Deutsche Telekom Laboratories, Technische Universität Berlin
Ernst-Reuter-Platz 7, 10587 Berlin, Germany
{jens.ahrens,sascha.spors}@telekom.de

ABSTRACT

Sound field reproduction methods like higher order Ambisonics which are based on orthogonal expansions always introduce a limitation of the spatial bandwidth of the secondary source driving function. This spatial truncation creates a sweet spot in the center of the secondary source distribution. This spot, or rather area, is "sweet" both in terms of spatial aliasing artifacts as well as in terms of accuracy of the desired component of the reproduced wave field. The higher the temporal frequency of the reproduced wave field the smaller is the sweet spot. In this paper we show that the location sweet spot can be moved freely inside the secondary source distribution. The accuracy of the actual reproduced wave field is then significantly higher in the sweet spot than in the same region in the conventional approach.

Index Terms— Higher order Ambisonics, sweet spot, Fourier series, spatial aliasing

1. INTRODUCTION

Wave field reproduction methods aiming at the reproduction over an extended receiver area typically employ a high number of loudspeakers which surround the receiver area. Due to the physical properties of practical implementations, artifact-free reproduction can not be achieved. When numerical methods are employed as e.g. in [1], the reproduction can be optimized with respect to a target area commonly referred to as *sweet spot*. The location of this sweet spot can be chosen with some amount of freedom. However, numerical approaches are computationally expensive and give only little insight into the properties of the actual reproduced wave field.

Analytical approaches are typically significantly beneficial both in terms of computational complexity as well as in terms of interpretability of the results. However, the target area with respect to which the reproduction is optimized is confined to the center of the loudspeaker array. In this paper, we extend the analytical approach presented by the authors in [2, 3] such that the sweet spot can be freely positioned inside the secondary source distribution (i.e. the loudspeaker array).

Note that we do not consider wave field synthesis (WFS) in this paper. This is due to the fact that WFS as commonly implemented does not exhibit a pronounced sweet spot. It is rather such that spatial aliasing is spread over the entire receiver area for higher frequencies [3].

2. NOMENCLATURE

For convenience, we restrict our considerations to two spatial dimensions. This means in this context that a wave field under consideration is independent from one of the spatial coordinates,

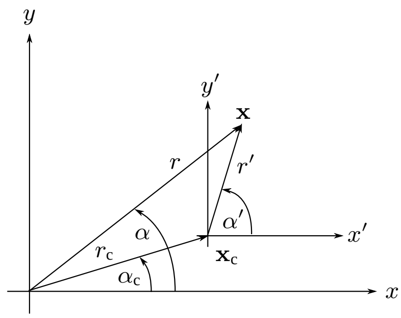

Fig. 1. The coordinate system used in this paper. The center of the secondary source distribution coincides with the origin of the global coordinate system. The prime $'$ denotes quantities belonging to a local coordinate system with origin $\mathbf{x}_c$ (refer to section 4.1).

i.e. $P(x, y, z, \omega) = P(x, y, \omega)$. The two-dimensional position vector in Cartesian coordinates is given as $\mathbf{x} = [x\ y]^T$. The Cartesian coordinates are linked to the polar coordinates via $x = r\ \cos\alpha$ and $y = r\ \sin\alpha$. Refer to the coordinate system depicted in figure 1.

The acoustic wavenumber is denoted by k. It is related to the temporal frequency by $k^2 = \left(\frac{\omega}{c}\right)^2$ with ω being the radial frequency and c the speed of sound. Outgoing monochromatic plane and cylindrical waves are denoted by $e^{-j\frac{\omega}{c}r\cos(\theta_{pw}-\alpha)}$ and $H_0^{(2)}(\frac{\omega}{c}r)$ respectively, with θ_{pw} being the propagation direction of the plane wave. The imaginary unit is denoted by j ($j = \sqrt{-1}$).

3. GENERAL FORMULATION

In this section, we briefly review the general approach presented by the authors in [2, 3]. Its physical fundament is the so-called *simple source approach* and it can be seen as an analytical formulation of what is known as higher order Ambisonics. The simple source approach for interior problems states that the acoustic field generated by events outside a volume can also be generated by a continuous distribution of secondary simple sources enclosing the respective volume [4].

As stated in section 2, we limit our derivations to two-dimensional reproduction for convenience. Furthermore, we assume the distribution of secondary sources to be circular. In order to fulfill the requirements of the simple source approach and therefore for artifact-free reproduction, the wave fields emitted by the secondary sources have to be two-dimensional. We thus have to assume a continuous circular distribution of secondary line sources positioned perpendicular to the target plane (the receiver plane) [4]. Our approach is there-

fore not directly implementable since loudspeakers exhibiting the properties of line sources are commonly not available. Real-world implementations usually employ loudspeakers with closed cabinets as secondary sources. The properties of these loudspeakers are more accurately modeled by point sources.
The main motivation to focus on two dimensions is to keep the mathematical formulation simple in order to illustrate the general principle of the presented approach. The extension both to three-dimensional reproduction (i.e. spherical arrays of secondary point sources) and to two-dimensional reproduction employing circular arrangements of secondary point sources is straightforward and can be found e.g. in [2].

3.1. Derivation of the secondary source driving function

The reproduction equation for a continuous circular distribution of secondary line sources and with radius r_0 centered around the origin of the coordinate system is given by

$$P(\mathbf{x},\omega) = \int_0^{2\pi} D(\alpha_0,\omega)\, G_{\text{2D}}(\mathbf{x}-\mathbf{x}_0,\omega)\, r_0\, d\alpha_0 \;, \tag{1}$$

where $\mathbf{x}_0 = r_0 \cdot [\cos\alpha_0 \;\; \sin\alpha_0]^T$. $P(\mathbf{x},\omega)$ denotes the reproduced wave field, $D(\alpha_0,\omega)$ the driving function for the secondary source situated at $\mathbf{x}_0$, and $G_{\text{2D}}(\mathbf{x}-\mathbf{x}_0,\omega)$ its two-dimensional spatio-temporal transfer function.
A fundamental property of (1) is its inherent non-uniqueness and ill-posedness [5]. I.e. in certain situations, the solution is undefined and so-called *critical* or *forbidden frequencies* arise. The forbidden frequencies are discrete and represent the resonances of the cavity under consideration. However, there are indications that the forbidden frequencies are only of minor relevance when practical implementations are considered [4].
Equation (1) constitutes a circular convolution and therefore the convolution theorem

$$\mathring{P}_\nu(r,\omega) = 2\pi r_0\, \mathring{D}_\nu(\omega)\, \mathring{G}_\nu(r,\omega) \tag{2}$$

applies [6]. $\mathring{P}_\nu(r,\omega)$, $\mathring{D}_\nu(\omega)$, and $\mathring{G}_\nu(r,\omega)$ denote the Fourier series expansion coefficients of $P(\mathbf{x},\omega)$, $D(\alpha,\omega)$, and $G_{\text{2D}}\left(\mathbf{x}-[r_0\; 0]^T\right)$[1].
The Fourier series expansion coefficients $\mathring{F}_\nu(r,\omega)$ of a two-dimensional function $F(\mathbf{x},\omega)$ can be obtained via [4]

$$\mathring{F}_\nu(r,\omega) = \frac{1}{2\pi}\int_0^{2\pi} F(\mathbf{x},\omega)e^{-j\nu\alpha}\, d\alpha \;. \tag{3}$$

The function $F(\mathbf{x},\omega)$ can then be synthesized as

$$F(\mathbf{x},\omega) = \sum_{\nu=-\infty}^{\infty} \mathring{F}_\nu(r,\omega)\, e^{j\nu\alpha} \;. \tag{4}$$

For propagating wave fields the coefficients $\mathring{F}_\nu(r,\omega)$ can be decomposed as

$$\mathring{F}_\nu(r,\omega) = \breve{F}_\nu(\omega) J_\nu\left(\frac{\omega}{c}r\right) \;, \tag{5}$$

whereby $J_\nu(\cdot)$ denotes the ν-th order Bessel function [4].
From (2) and (5) we can deduce that

$$\mathring{D}_\nu(\omega) = \frac{1}{2\pi r_0}\,\frac{\mathring{P}_\nu(r,\omega)}{\mathring{G}_\nu(r,\omega)} = \tag{6}$$

$$= \frac{1}{2\pi r_0}\,\frac{\breve{P}_\nu(\omega)\cdot J_\nu\left(\frac{\omega}{c}r\right)}{\breve{G}_\nu(\omega)\cdot J_\nu\left(\frac{\omega}{c}r\right)} \tag{7}$$

For $J_\nu\left(\frac{\omega}{c}r\right) \neq 0$ the Bessel functions in (7) cancel out directly. Wherever $J_\nu\left(\frac{\omega}{c}r\right) = 0$ de l'Hôpital's rule [7] can be applied to proof that the Bessel functions also cancel out in these cases, thus making $\mathring{D}_\nu(\omega)$ and therefore also $D(\alpha_0,\omega)$ independent from the receiver position.
Introducing the result into (4) finally yields the secondary source driving function $D(\alpha_0,\omega)$ for a secondary source situated at position $\mathbf{x}_0$ reproducing a desired wave field with expansion coefficients $\breve{P}_\nu(\omega)$ reading

$$D(\alpha,\omega) = \frac{1}{2\pi r_0}\sum_{\nu=-\infty}^{\infty}\frac{\breve{P}_\nu(\omega)}{\breve{G}_\nu(\omega)}e^{j\nu\alpha} \;, \tag{8}$$

whereby we omitted the index 0 in α_0 for convenience.
We assume monopole line sources in the remainder of this paper for convenience. The two-dimensional free-field Green's function $G_{\text{2D}}(\mathbf{x}-\mathbf{x}_0,\omega)$ representing the spatio-temporal transfer function of a secondary source at position $\mathbf{x}_0$ is then the zero-th order Hankel function of second kind $H_0^{(2)}\left(\frac{\omega}{c}\left|\mathbf{x}-\mathbf{x}_0\right|\right)$ [4].
Equation (8) can be verified by inserting it into (1). After introducing the Fourier series expansion of the secondary source wave fields according to (4), exchanging the order of integration and summation, and exploitation of the orthogonality of the circular harmonics $e^{j\nu\alpha}$ [4] one arrives at the Fourier series expansion of the desired wave field, thus proving perfect reproduction. Note however that the coefficients $\breve{P}_\nu(\omega)$ respectively $\breve{G}_\nu(\omega)$ are typically derived from interior expansions. This implies that the desired wave field is only correctly reproduced inside the secondary source distribution.

3.2. Properties of the reproduced wave field

For the theoretic continuous secondary source distribution, any wave field which is source-free inside the secondary source distribution can be perfectly reproduced apart from the forbidden frequencies (refer to section 3.1).
Real-world implementations of audio reproduction systems will always employ a finite number of discrete secondary sources. This spatial discretization constitutes spatial sampling and results in spatial aliasing. In this section, we briefly review the consequences of spatial sampling. A thorough treatment can be found in [3, 8].
It can be shown that the angular sampling of the driving function results in repetitions of the angular spectrum of the continuous driving function $\mathring{D}_\nu(\omega)$ [8]

$$\mathring{D}_{\nu,S}(\omega) = \sum_{\eta=-\infty}^{\infty}\mathring{D}_{\nu+\eta L}(\omega) \;, \tag{9}$$

when L equiangular sampling points (i.e. loudspeakers) are taken. Equation (2) states that the angular spectrum of the reproduced wave field $\mathring{P}_\nu(r,\omega)$ is equal to the angular spectrum of the driving function $\mathring{D}_\nu(\omega)$ weighted by the angular spectrum of the secondary sources $\mathring{G}_\nu(r,\omega)$. Note that all angular spectra are taken with respect to the expansion around the origin of the global coordinate system.

[1] Note that the coefficients $\mathring{G}_\nu(r,\omega)$ as used throughout this paper assume that the secondary source is situated at the position $(r = r_0, \alpha = 0)$ and is orientated towards the coordinate origin.

In order to yield the angular spectrum $\mathring{P}_{\nu,S}(r,\omega)$ of the wave field reproduced by a discrete secondary source distribution, the spectral repetitions given by (9) have to be introduced into (2). The case of $\eta = 0$ then describes the desired component of the reproduced wave field. The cases of $\eta \neq 0$ describe additional components due to sampling. Note that these additional components can not be avoided.
In order to further investigate the properties of the wave field reproduced by a discrete secondary source distribution, we have to choose a sample scenario. For convenience, we assume a distribution of $L = 56$ secondary monopole line sources reproducing a monochromatic plane wave with propagation direction $\theta_{\text{pw}} = \frac{3\pi}{2}$. In this case $\breve{G}_\nu(\omega) = \frac{j}{4} H_\nu^{(2)}\left(\frac{\omega}{c} r_0\right)$ and $\breve{P}_\nu(\omega) = j^{-\nu} e^{-j\nu\theta_{\text{pw}}}$ [4, 9].
The Fourier coefficients $\mathring{D}_\nu(\omega)$ of the continuous driving function for the above described scenario are illustrated in figure 2(b). It can be seen that $\mathring{D}_\nu(\omega)$ is not bandlimited with respect to the angular frequency ν. Thus, when the angular bandwidth of the driving function is not artificially limited, the angular repetitions overlap and interfere.
In order to avoid such overlapping and interference of the spectral repetitions, the angular bandwidth of the continuous driving function can be limited as

$$D_N(\alpha,\omega) = \frac{1}{2\pi r_0} \sum_{\nu=-N}^{N} \frac{\breve{P}_\nu(\omega)}{\breve{G}_\nu(\omega)} e^{j\nu\alpha} , \qquad (10)$$

whereby $N = \frac{L-1}{2}$ when a discrete distribution of an odd number L of secondary sources is considered and accordingly for even L. Strictly spoken, when (10) is applied spatial aliasing is prevented since no spectral overlaps occur. However, since the spatial spectrum $\mathring{G}_\nu(r,\omega)$ of the secondary sources is not bandlimited, spatial repetitions of the driving function will always be reproduced. Refer to figure 2(a). Although this is rather a reconstruction error [3] it is commonly also referred to as spatial aliasing. We do so as well in the remainder for convenience.
The band-limitation according to (10) keeps the center of the secondary source setup free of aliasing artifacts [3]. However, as a consequence of this spectral band-limitation, the spatial bandwidth of the desired component of the reproduced wave field is also limited. The energy of the desired component of the reproduced wave field concentrates around the center of the secondary source distribution especially for high temporal frequencies. Compare figures 3(a) and 3(b). I.e., wave fields with high temporal frequency content can not be reproduced farther away from the array center than a certain critical distance with such a spatially bandlimited driving function. In other words, the above described approach of sound field reproduction exhibits a pronounced sweet spot in the center of the secondary source distribution both in terms of spatial aliasing artifacts as well as in terms of accuracy of the desired component of the reproduced wave field.
Note that increasing the spatial bandwidth of the driving function does indeed increase the spatial bandwidth of the desired component of the reproduced wave field. However, it also significantly increases spatial aliasing.

4. MOVING THE SWEET SPOT

It will be shown in the following that the system inherent sweet spot can be moved by limiting the spatial bandwidth of the desired wave field $P(\mathbf{x},\omega)$ with respect to an expansion center other that the center of the secondary source distribution. The sweet spot then coincides with this new expansion center.

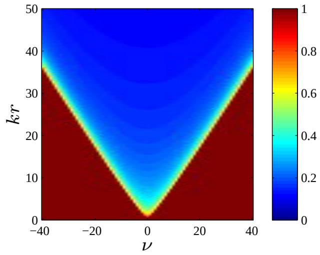

(a) Secondary source transfer function $\left|\mathring{G}_\nu(r,\omega)\right|$

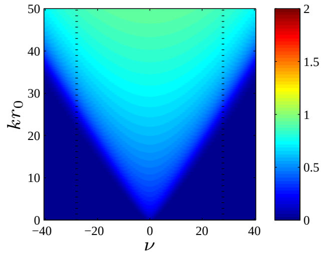

(b) Continuous conventional driving function $\left|\mathring{D}_\nu(\omega)\right|$

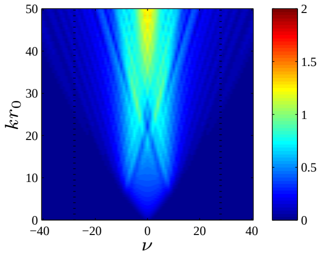

(c) Continuous driving function $\left|\mathring{D}_{\text{c},\nu}(\omega)\right|$ for a desired wave field spatially band-limited around the expansion center $\mathbf{x}_\text{c} = (1, 0)$, $M = 12$.

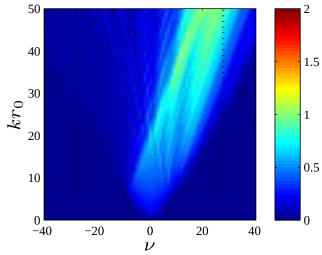

(d) Continuous driving function $\left|\mathring{D}_{\text{c},\nu}(\omega)\right|$ for a desired wave field spatially band-limited around the expansion center $\mathbf{x}_\text{c} = (1, \frac{\pi}{4})$, $M = 12$.

Fig. 2. Absolute values of the Fourier coefficients with respect to the expansion around the origin of the global coordinate system. The black dotted lines indicate the interval of one spectral repetition due to spatial sampling. $kr_0 = 50$ corresponds to $f \approx 2700$ Hz.

4.1. Limiting the spatial bandwidth of the desired wave field with respect to a given expansion center

The desired wave field $P(\mathbf{x},\omega)$ can be expanded around any arbitrary expansion center $\mathbf{x}_\text{c}$. With (4) and (5) and when $P(\mathbf{x},\omega)$ is bandlimited with bandwidth $2M+1$ around $\mathbf{x}_\text{c}$, this expansion is given by

$$P_M(\mathbf{x},\omega) = \sum_{\mu=-M}^{M} \breve{P}_\mu(\omega) J_\mu\left(\frac{\omega}{c} r'\right) e^{j\mu\alpha'} . \qquad (11)$$

r' and α' denote the position coordinates with respect to a local coordinate system whose origin is at $\mathbf{x}_\text{c}$ and whose axes are parallel to those of the global coordinate system in r and α. Refer to figure 1. Note that $r' = r'(\mathbf{x})$ and $\alpha' = \alpha'(\mathbf{x})$.
However, for the calculation of the driving function (10) we require the coefficients $\breve{P}_\nu(\omega)$ with respect to the expansion around the origin of the global coordinate system. We therefore introduce the addition theorem for cylinder harmonics [9] into (11) to yield

$$P_M(\mathbf{x},\omega) = \sum_{\nu=-\infty}^{\infty} J_\nu\left(\frac{\omega}{c} r\right) e^{j\nu\alpha} \times \\ \times \underbrace{\sum_{\mu=-M}^{M} \breve{P}_\mu(\omega) J_{\nu-\mu}\left(\frac{\omega}{c} r_\text{c}\right) e^{-j(\nu-\mu)\alpha_\text{c}}}_{=\breve{P}_{\nu,M}(\omega)} . \qquad (12)$$

For plane waves $\breve{P}_\mu(\omega) = j^{-\mu} e^{-j\mu\theta_{\text{pw}}}$.
To reproduce $P_M(\mathbf{x},\omega)$, the expansion coefficients $\breve{P}_{\nu,M}(\omega)$ are in-

troduced into (10). Therefore, two spatial bandlimitations are apparent:

(A) $P_M(\mathbf{x}, \omega)$ is bandlimited with respect to an expansion around $\mathbf{x}_c$. The bandlimit is denoted by M. From (12) it can be deduced that $P_M(\mathbf{x}, \omega)$ nevertheless exhibits infinite spatial bandwidth with respect to an expansion around the coordinate origin.

(B) The driving function $D_N(\alpha, \omega)$ (equation (10)) is bandlimited with respect to an expansion around the coordinate origin. The bandlimit is denoted by N. The desired component of the reproduced wave field is bandlimited in both senses.

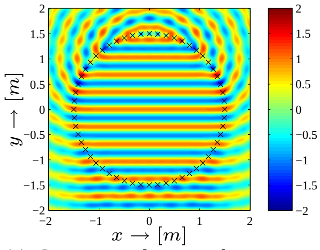

(a) Conventional approach. $f_{\text{pw}} = 1000$ Hz. The spatial bandlimit is $N = 27$.

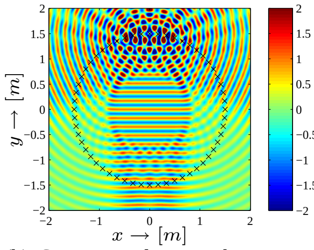

(b) Conventional approach. $f_{\text{pw}} = 2000$ Hz. The spatial bandlimit is $N = 27$.

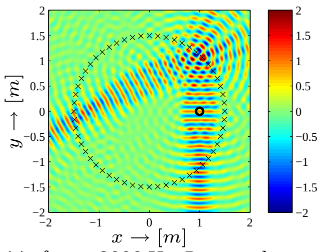

(c) $f_{\text{pw}} = 2000$ Hz. Presented approach with expansion center $\mathbf{x}_c = (1, 0)$. The spatial bandlimits are $N = 56$ and $M = 12$.

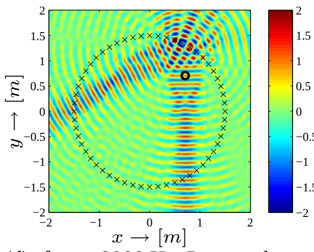

(d) $f_{\text{pw}} = 2000$ Hz. Presented approach with expansion center $\mathbf{x}_c = (1, \frac{\pi}{4})$. The spatial bandlimits are $N = 56$ and $M = 12$.

Fig. 3. Wave fields reproduced by a circular distribution of $L = 56$ discrete loudspeakers and with radius $r_0 = 1.5$ m reproducing a plane wave with propagation direction $\theta_{\text{pw}} = \frac{3\pi}{2}$. The marks indicate the positions of the secondary sources.

4.2. Spatial aliasing properties

The spatial bandwidth limitation introduced in section 4.1 leads to favorable spatial aliasing properties as described in this section.

In figures 2(c) and 2(d) it can be seen that the energy of the angular spectrum $\mathring{D}_{c,\nu}(\omega)$ of the continuous proposed driving function is distributed such that either (I) the spectral repetitions due to spatial sampling overlap only in regions of low energy (refer to figures 2(c) and 3(c)) or (II) the overlaps of the spectral repetitions do not lead to interference of high energy components (refer to figures 2(d) and 3(d)). This enables the application of a driving function (10) with a bandlimit N significantly higher than $N = \frac{L-1}{2}$ in the conventional approach and therefore leads to a higher spatial bandwidth of the desired component of the reproduced wave field with only a little amount of aliasing. Two examples of the application of the proposed driving function are shown in figures 3(c) and 3(d). It can be seen that sweet spots form around the expansion centers $\mathbf{x}_c$ marked by the small circles. Outside the sweet spots strong deviations from the desired wave field arise. Like in the conventional approach, the sweet spots get smaller with increasing temporal frequency of the reproduced wave field.

When comparing figures 3(c) and 3(d) to the application of the conventional driving function illustrated in figure 3(b), it can be seen that due to the wider bandwidth of the driving function, the proposed approach indeed enables the reproduction of the desired wave field in locations where the conventional approach fails to do so. The reproduction can thus be optimized with respect to a given - potentially dynamic - target area.

5. CONCLUSIONS

In this paper we presented an analytical approach to sound field reproduction with a movable sweet spot. Conventional analytical approaches inherently exhibit a static sweet spot in the center of the secondary source distribution. The farther away the receiver is from the center of the secondary source distribution, the less accurate is the desired component of the reproduced wave field and the more spatial aliasing artifacts are present.

When the wave field to be reproduced is spatially bandlimited with respect to the expansion around an arbitrary point inside the secondary source distribution, then the spatial bandwidth of the secondary source driving function can be significantly higher than in the conventional approach while spatial aliasing is still kept low. As a consequence, the desired wave field can be reproduced in locations where the conventional approach fails to do so. A sweet spot both in terms of accuracy of the desired component of the reproduced wave field as well as in terms of spatial aliasing artifacts is created around the expansion center with respect to which the wave field to be reproduced is bandlimited. Inside this sweet spot the reproduction is significantly more accurate than in the conventional approach. Outside the sweet spot the reproduced wave field can deviate strongly from the desired one. This is the case for both the conventional as well as for the proposed approach.

It could not be clarified within the scope of this paper, how well the presented approach performs in terms of accuracy compared to numerical methods like [1]. However, its entirely analytical character suggests that it is significantly beneficial in terms of computational complexity. Furthermore, it allows for an analytical investigation of the properties of the actual reproduced wave field. The general physical limitations of the involved loudspeaker setups can be determined no matter if the latter are driven by analytical or numerical methods.

6. REFERENCES

[1] O. Kirkeby and P.A. Nelson, "Reproduction of plane wave sound fields," *JASA*, vol. 94, no. 5, pp. 2992–3000, Nov. 1993.

[2] J. Ahrens and S. Spors, "An analytical approach to sound field reproduction using circular and spherical loudspeaker distributions," *Acta Acustica utd. with Acustica*, vol. 94, no. 6, pp. 988–999, Nov./Dec. 2008.

[3] S. Spors and J. Ahrens, "A comparison of wave field synthesis and higher-order Ambisonics with respect to physical properties and spatial sampling," in *125th Conv. of the AES*, San Francisco, CA, Oct. 2–5 2008.

[4] E.G. Williams, *Fourier Acoustics: Sound Radiation and Nearfield Acoustic Holography*, Academic Press, London, 1999.

[5] L.G. Copley, "Fundamental results concerning integral representations in acoustic radiation," *JASA*, vol. 44, pp. 28–32, 1968.

[6] B. Girod, R. Rabenstein, and A. Stenger, *Signals and Systems*, J.Wiley & Sons, 2001.

[7] E.W. Weisstein, "L'Hospital's Rule. MathWorld – A Wolfram Web Resource.," http://mathworld.wolfram.com/LHospitalsRule.html.

[8] S. Spors and R. Rabenstein, "Spatial aliasing artifacts produced by linear and circular loudspeaker arrays used for wave field synthesis," in *120th Convention of the AES, Paris, France*, May 20–23 2006.

[9] Milton Abramowitz and Irene A. Stegun, Eds., *Handbook of Mathematical Functions*, Dover Publications Inc., New York, 1968.